International Journal of Greenhouse Gas Control 77 (2018) 82–87

Contents lists available at ScienceDirect

International Journal of Greenhouse Gas Control

journal homepage: www.elsevier.com/locate/ijggc

Optimum storage depths for structural CO_2 trapping

Stefan Iglauer*

Edith Cowan University, School of Engineering, 270 Joondalup Drive, 6027 Joondalup, Australia

ARTICLE INFO

Keywords:
CO_2 geo-sequestration
Structural trapping
Storage capacity
CO_2 mass
Wettability
Buoyancy
Optimal storage depth
CO_2-brine density reversal

ABSTRACT

Structural trapping is the primary CO_2 geo-storage mechanism, and it has historically been quantified by CO_2 column heights, which can be permanently immobilized beneath a caprock, using a buoyancy force-capillary force balance. However, the high dependence of CO_2-wettability (a key parameter in the above analysis) on pressure and temperature – and thus storage depth – has not been taken into account. Importantly, rock can be CO_2-wet at high pressure, and this wettability reversal results in zero structural trapping below a certain storage depth (~2400 m maximum caprock depth for a most likely scenario is estimated here). Furthermore, more relevant than the CO_2 column height is the actual mass of CO_2 which can be stored by structural trapping (m_{CO2}). This aspect has now been quantified here, and importantly, m_{CO2} goes through a maximum at ~1300 m depth, thus there exists an optimal storage depth at around 1300 m depth.

1. Introduction

Carbon Geo-Sequestration (CGS) has been identified as a key technology to cut anthropogenic greenhouse gas emissions and thus mitigate climate change (Lackner, 2003; Intergovernmental Panel on Climate Change (IPCC, 2005; Orr, 2009). In CGS, CO_2 is captured from large point-source emitters and injected deep underground into geologic formations for disposal.

In this context structural trapping is a key mechanism which keeps the buoyant CO_2 – the CO_2 has a lower density than the resident formation brine and thus migrates upwards (Span and Wagner, 1996) – trapped in the subsurface (Intergovernmental Panel on Climate Change (IPCC, 2005; Naylor et al., 2011; Iglauer et al., 2015a). Structural trapping requires a tight, impermeable caprock (typically shale), which seals the upper boundary of the storage formation so that CO_2 cannot pass (Broseta, 2012). However, caprock is – although very tight – also porous and thus in principle allows CO_2 to percolate through it (e.g. cp. Dewhurst et al., 2002; Armitage et al., 2013; Wollenweber et al., 2010; Song and Zhang, 2013; Busch et al., 2008; Li et al., 2006). Despite this porosity it has been proposed that capillary forces (which are determined at the molecular level, De Gennes et al., 2004) are sufficiently strong and prevent the buoyant CO_2 from moving upwards (into and through the caprock). This mechanism relies on the very small pores in the pore network of the caprock (5–100 nm for shale caprock; Nelson, 2009), which result in high CO_2 percolation pressures (i.e. the CO_2 pressure when CO_2 completely percolates and can flow through the caprock is very high, Thompson et al., 1987). The storage capacity of a caprock in terms of how much CO_2 pressure it can hold, and thus how much CO_2 in total it can store, can be quantified by a capillary force-buoyancy force balance (Eqs. (1)–(3)). Precisely, the buoyancy pressure p_b exerted by the CO_2 plume (Eq. (1)) has to be counterbalanced by the capillary pressure p_c (Eq. (2)); thus by equalizing p_b and p_c the CO_2 column height h which can be permanently immobilized beneath the caprock can be predicted (Naylor et al., 2011; Iglauer et al., 2012, 2015a; Arif et al., 2016a):

$$p_b = \Delta\rho g h \tag{1}$$

$$p_c = \frac{2\gamma\cos\theta}{r} \tag{2}$$

$$h = \frac{2\gamma\cos\theta}{\Delta\rho g r} \tag{3}$$

where γ is the CO_2-brine interfacial tension, θ is the brine – CO_2-rock contact angle (which quantifies the caprock's wettability), $\Delta\rho$ is the CO_2-brine density difference, g is the gravitational constant and r is the (average) pore radius of the caprock. Note that Eq. (3) is based on the assumption that the rock pores can be modelled as circular capillary tubes which have a contant radius. Eq. (3) is thus an approximation and different pore geometries will change the capillary pressure (Eq. (2), Crisp and Thorpe (1948), Espinoza and Santamarina (2017).

Although above aspects are relatively well-established, only recently major advances have been made with respect to the caprock's wettability (as expressed by the CO_2-water-caprock contact angle θ in Eqs. (2) and (3); Broseta et al., 2012; Iglauer et al., 2015a,b; Iglauer,

* Corresponding author.
E-mail address: s.iglauer@ecu.edu.au.

https://doi.org/10.1016/j.ijggc.2018.07.009
Received 25 July 2017
Available online 15 August 2018

Nomenclature

p	Pressure [Pa]
p_b	Buoyancy pressure [Pa]
p_c	Capillary pressure = pressure between wetting and non-wetting phase [Pa], i.e. pressure between CO_2 and brine phase
ρ	Density [kg/m^3]
ρ_{water}	Density of water [kg/m^3]
ρ_{CO2}	CO_2 density [kg/m^3]
Δρ	Density difference between water and CO_2 [kg/m^3]
h	CO_2 plume height permanently immobilized by structural trapping [m]
d	Depth [m]
θ	Water contact angle [°]
γ	Interfacial tension [N/m]
r	Pore radius [m]
T	Temperature [°C]
g	Gravitational constant [m/s^2]
ϕ	Porosity [-]
CO_2	Carbon dioxide
NaCl	Sodium chloride
TOC	Total organic content [ppm]
sc	Supercritical
A	Surface area of 3D CO_2 plume projected onto earth's surface [m^2]
m_{CO2}	Mass of CO_2 stored by structural trapping [kg]
R^2	coefficient of determination

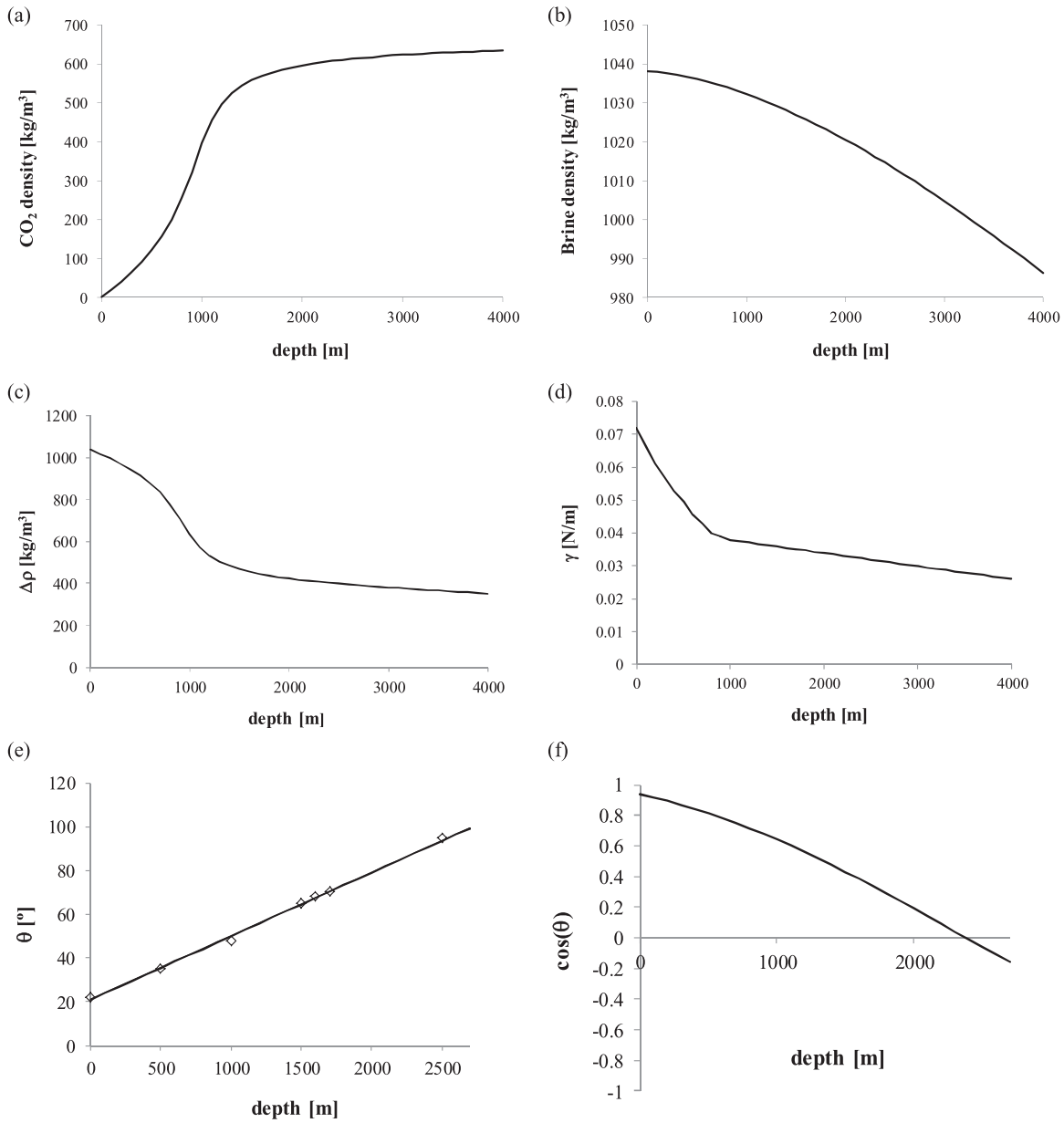

Fig. 1. Parameters required for structural trapping capacity assessment; (a) CO_2 density, (b) brine density, (c) CO_2-brine density difference Δρ, (d) CO_2-brine interfacial tension γ, (e) CO_2-brine-caprock contact angle θ, (f) cos(θ) – all parameters are plotted against depth to illustrate the inherent dependencies.

2017), and this has major implications for structural CO_2 storage capacities as outlined here. Of vital importance is the existence of a maximum storage depth below which structural trapping fails (i.e. CO_2 percolates upwards through the caprock), this is due to wettability reversal. Thus CGS by structural trapping is not feasible anymore below this depth, this is discussed in more detail below.

Furthermore, and importantly, not the CO_2 column height h (Eq. (3); Naylor et al., 2011; Iglauer et al., 2012, 2015a,b; Arif et al., 2016a) is the key parameter, instead the mass of CO_2 (or number of moles of CO_2 if you prefer) which can be stored is much more relevant. For simplicity, let's call this mass m_{CO2}. This is further outlined and discussed in detail below, but it is clear that m_{CO2} goes through a maximum at ~1300 m depth, thus there exists an optimum storage depth for structural trapping.

2. Structural trapping evaluation

Based on Eq. (3), there are three key quantities (γ, $\Delta\rho$, θ) which significantly vary with depth. This is displayed in Fig. 1 and briefly summarized here. The below analysis is based on the assumption that highly purified CO_2 is disposed, and 10 MPa/km hydrostatic and 30 K/km geothermal gradients exist. These temperature and pressure gradients reflect the common situation in deep saline storage aquifers (Meckel, 2010) and generally subsurface earth (Dake, 1978). However, temperatures and pressures in specific formations may deviate from those expectations due to their particular geologic history (e.g. over pressurization caused by tectonic compression), Chilingarian et al., 2002. The evaluation presented here thus focuses on the typically encountered conditions, and the limitations of the associated model developed here are discussed in a later Section (2.6) below.

2.1. The CO_2-water density difference $\Delta\rho$

$\Delta\rho$ is mainly driven by the significant change in CO_2 density (ρ_{CO2}) with depth d (due to the high CO_2 compressibility, Span and Wagner, 1996). Precisely, ρ_{CO2} increases drastically with depth (Fig. 1a), and reaches a pseudo-maximum at ~630 kg/m^3 (Span and Wagner, 1996), while water density slowly, but continuously decreases (Span and Pruss, 2002). Note that ρ_{water} = 1040 kg/m^3 at atmospheric conditions is used here for the analysis, i.e. the density of saline brine, e.g. compare Bachu and Adams (2003). This is approximately equivalent to a 1.5 M NaCl brine, an average salinity in the subsurface. However, salinity can strongly vary in the subsurface, from low values (500 ppm) to maximum saturations (e.g. ~350,000 ppm), Xie et al. (2006). $\Delta\rho$, γ, and particularly θ (Al-Yaseri et al., 2016a; Iglauer et al., 2015b; Iglauer, 2017) thus need to be adjusted for diverging salinities as these parameters depend on salinity. Overall, however, $\Delta\rho$ – which mirrors ρ_{CO2} versus d (Fig. 1b) – reaches a pseudo minimum at ~325 kg/m^3. Interestingly, at great depth (~15 km), density reversal occurs, i.e. at this depth CO_2 is heavier than water. This is discussed further in the implications section.

The $\Delta\rho$ function versus depth was fitted with a spline:

if $d \in$ [0;1000 m], then

$$\Delta\rho = -0.0003\ d^2 - 0.0663\ d + 1027.9$$

$$R^2 = 0.9976$$

if $d \in$ [1000 m; 1900 m], then

$$\Delta\rho = -(4 \times 10^{-7})\ d^3 + 0.002\ d^2 - 3.4116\ d + 2465.9$$

$$R^2 = 0.9992$$

if $d \in$]1900 m; 4000 m], then

$$\Delta\rho = -0.0363\ d + 492.64$$

$$R^2 = 0.9865$$

2.2. The CO_2-water interfacial tension γ

γ rapidly decreases with pressure, particularly for pressures (p) below the critical CO_2 pressure (p_{crit} = 7.3773 MPa, Span and Wagner, 1996). However, γ increases with increasing temperature, but this increase is less dramatic then the decrease in γ with p (Chalbaud et al., 2009; Chun and Wilkinson, 1995; Hebach et al., 2002; Bennion and Bachu, 2007; Li et al., 2012a,b; Georgiadis et al., 2010; Park et al., 2005; Arif et al., 2016a,b,c). Thus γ overall decreases significantly with depth (Fig. 1d), also cp. Meckel (2010).

Again the curve is fitted with a spline:if $d \in$ [0;900 m], then

$$\gamma = (3 \times 10^{-8})\ d^2 - (6 \times 10^{-5})\ d + (0.072)$$

$$R^2 = 0.9963$$

if $d \in$]900 m; 4000 m], then

$$\gamma = (6 \times 10^{-10})\ d^2 - (7 \times 10^{-6})\ d + 0.0451$$

$$R^2 = 0.9735$$

2.3. The CO_2-water-rock contact angle θ

A tremendous amount of work has gone into measuring the water-rock-CO_2 contact angle θ in recent years (e.g. Chiquet et al., 2007; Broseta et al., 2012; Al-Yaseri et al., 2016a,b; Arif et al., 2016a,b; Espinoza and Santamarina, 2010; Farokhpoor et al., 2013; Li et al., 2007; Saraji et al., 2013; Iglauer et al., 2014,2015a,b; Iglauer, 2017; Sarmadivaleh et al., 2015; Jung and Wang, 2012; Yang et al., 2008; Shojai Kaveh et al., 2014, 2016; Chen et al., 2015; Guiltinan et al., 2017), so that the relationship between θ and depth can be derived (Fig. 1e). However, data is scarce for real caprock; thus real caprock data from (Iglauer et al., 2015a), measured at reservoir conditions is used while considering Iglauer et al. (2014); Chaudhary et al. (2015); Roshan et al. (2016); Shojai Kaveh et al. (2016) and Al-Yaseri et al.'s (2016a,b, 2017) measurements. Several important points need to be made: θ increases drastically with increasing pressure (for all rocks due to increasing intermolecular CO_2-rock interactions (Iglauer et al., 2012; Iglauer, 2017; Arif et al., 2016b; Chen et al., 2015; Liang et al., 2017), and significantly with increasing temperature (when considering a caprock with a low organic content, Al-Yaseri et al., 2017; Arif et al., 2017). Most importantly, θ dramatically increases with increasing organic content, to the extent that rock can be completely CO_2-wet (i.e. $\theta = 180°$), (Dickson et al., 2006; Yang et al., 2008; Espinoza and Santamarina, 2010; Arif et al., 2016a,b, 2017; Iglauer et al., 2014, 2015a,b; Iglauer, 2017; Pan et al., 2018). For simplicity, a TOC (total organic content) of 1000 mg/kg (=0.1 wt%) is used here which was measured for the caprock tested by Iglauer et al. (2015a). However, for higher TOC – which is absolutely possible for shale (Vernik and Milovac, 2011) – θ is much higher (Arif et al., 2017), and thus the storage capacity is reduced accordingly; there is thus no doubt that TOC needs to be known for any reliable storage capacity assessment.

Following fit is obtained from the θ-versus-depth graph (Fig. 1e; $R^2 = 1$):

$$\theta = 0.029\ d + 20.962$$

Importantly, for the common geological scenario discussed here, below a depth of ~2400 m, cos(θ), and thus h turn negative (because of wettability reversal), Fig. 1f. Thus there is an expectation that for caprocks located at storage depths below ~2400 m, structural trapping will fail, unless the reservoir is significantly underpressurized. This is further discussed in the below CO_2 column height discussion.

2.4. CO_2 column height h

All variables required for calculating h (cp. Eq. (3)) as a function of depth have been derived above (r is taken as 50 nm, Nelson, 2009; and g is 9.81 m/s^2), thus h as a function of depth can be calculated via Eq. (3); Fig. 2a. The h-curve in this graph can be fitted with a spline:

if $h \in$ [0;500 m], then

$h = -0.1802\ d + 258.8$

$R^2 = 0.9828$

if $h \in$]500 m; 1200 m], then

$h = 0.0001\ d^2 - 0.1986\ d + 246.15$

$R^2 = 0.9582$

if $h \in$]1200 m; 4000 m], then

$h = -0.1453\ d + 346.49$

$R^2 = 0.9965$

h decreases with depth (Fig. 2a), but h has a local maximum at ~1300 m; and at ~2400 m reaches zero. Thus below ~2400 m structural trapping is predicted to fail (because of wettability reversal, cp. Fig. 1e,f); when considering common brine salinity and temperature- and pressure gradients. Possible deviations from these expectations are further discussed in Section 2.6.

2.5. The mass of CO_2 which can be stored by structural trapping

However, and importantly, h is actually not the key parameter, as it is much more relevant to know how much (i.e. which mass m_{CO2}) CO_2 can be stored (e.g. Intergovernmental Panel on Climate Change (IPCC, 2005; Firoozabadi and Cheng, 2010) – and this is quantified by

$$m_{CO2} = \rho_{CO2} h A \phi, \quad (4)$$

where ϕ is the reservoir (storage) rock porosity (here ϕ = 0.2 is assumed which is a common value for sandstones), and A is the average lateral CO_2-swept reservoir area; i.e. the lateral spread of the three-dimensional CO_2 plume averaged over its vertical height. The calculation of A requires a full-scale reservoir simulation, with which the exact 3D shape of the CO_2 plume can be predicted, and A can be derived (e.g. see Doughty, 2010; Gershenzon et al., 2015; Al-Khdheeawi et al., 2017). In addition, early in a CGS project more and more CO_2 accumulates beneath a caprock and CO_2 spreads out laterally (Hesse et al., 2008; Hesse and Woods, 2010), while CO_2 continuously dissolves in undersaturated formation brine which sinks deeply into the reservoir (Riaz et al., 2006); thus A is a transient parameter. Strictly speaking ρ_{CO2} is also an average, of the whole CO_2 plume as it changes with depth, but this is a relatively insignificant effect over a few hectometres at depth > 1500 m. While all these effects need to be considered, the maximum column height h is a constant in a given reservoir scenario, and it sets the upper boundary of the allowable CO_2 column height. However, h varies with depth (compare Fig. 2a), which significantly affects m_{CO2}. To illustrate this effect quantitatively, A is assumed here to be A = 100 m × 100 m = 10^4 m^2 (just as an example).

The resulting m_{CO2} is plotted versus depth in Fig. 2b, and the m_{CO2}-graph can be fitted via a spline:

if $m_{CO2} \in$ [0;1200 m], then

$m_{CO2} = (6 \times 10^{-5})\ d^2 + 0.0532\ d + 2.6281$

$R^2 = 0.9896$

if $m_{CO2} \in$]1200 m; 4000 m], then

$m_{CO2} = -0.1738\ d + 406.98$

$R^2 = 0.993$

The key point now is that m_{CO2} goes through a maximum at ~1300 m. Thus there exists an optimal CO_2 storage depth for structural trapping. Note that this depth estimate is independent of A.

2.6. Model validation

The proposed model was validated against 76 datasets observed for natural CO_2 reservoirs (Miocic et al., 2016). It was specifically assessed whether the maximum caprock depth predicted here (~2400 m) is consistent with the field data. However, a direct comparison is only possible for a few cases (7 cases thus 7/76 = 9.2% of all datasets) as only these contain pure CO_2 (i.e. CO_2 purity ≥ 99%). To consider the other reservoirs in this analysis (where CO_2 concentration ranges from 25 to 99%), the gas density can be adjusted by taking the actual CO_2 concentration into account, and Δρ, γ and θ can thus be estimated (Li et al., 2012a,b; Al-Yaseri et al., 2016a,b). These parameters also need to be adjusted for deviations from the typical geothermal and hydrostatic gradients (these gradients may be atypical, this is discussed in more detail in Section 2.7 below); so that the column height h for a corresponding high CO_2-purity reservoir can be determined (recall that when h = 0, this is the maximum caprock depth for storage). Thus, if the CO_2 concentration, and the specific reservoir pressure and temperature are taken into account, a direct comparison is possible.

Indeed, all data for the natural reservoirs (note that only measured field data was considered, i.e. the data in Miocic's table SI 1 marked with an asterisk was excluded, so 47 cases were considered here for the comparison) was consistent with the model proposed here, with two exceptions (2 out of 47 = 4.25%), namely the Jackson Dome and the Big Piney La Barge Highland. These two exceptional reservoirs have carbonate seals, which apparently creates a special sealing effect (see further discussion below in Section 2.7).

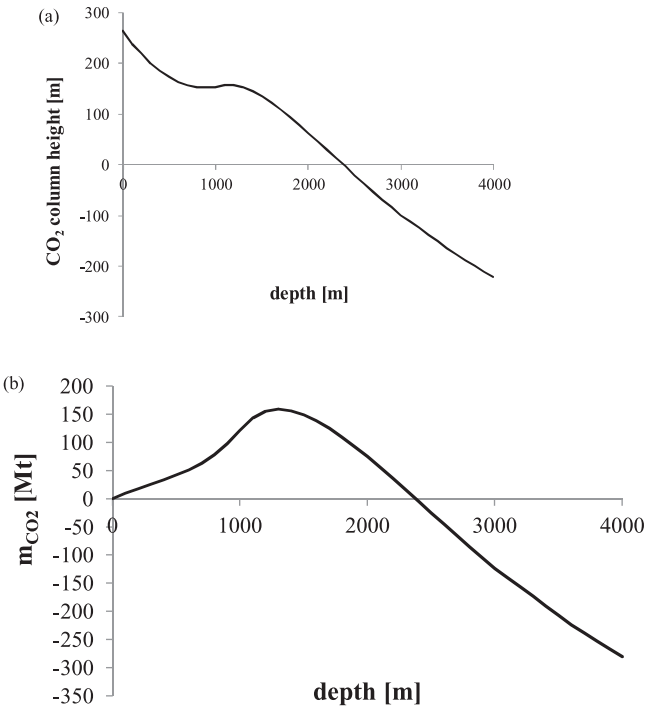

Fig. 2. Structural storage capacity assessment, (a) CO_2 column height h which can be permanently immobilized beneath the caprock, (b) mass of CO_2 (m_{CO2}) which can be stored by structural trapping.

2.7. Model limitations

As mentioned above the proposed model for predicting structural trapping capacities assumes typical geothermal and hydrostatic gradients and average brine salinities. The specific conditions may, however, deviate from such typical conditions, e.g. reservoir pressure can be over- or under pressurized (Akhbari and Hesse, 2016; Chilingarian et al., 2002). Thus the relevant model parameters ($\Delta\rho$, γ, θ) have to be adjusted accordingly. Furthermore, in case CO_2 is mixed with lighter gas (e.g. N_2), the capillary force-buoyancy force balance changes, and safe storage can be achieved at much greater depth as evidenced by various natural CO_2 reservoirs (Miocic et al., 2016). However, CO_2 storage capacity is of course reduced significantly in such a scenario.

It is moreover noted that there are some interesting exceptions, which are not covered by the model proposed here, namely the natural Jackson Dome and Big Piney La Barge Highland reservoirs contain 99% CO_2, at pressures of 45–53 MPa and temperatures of 74–90 °C (Miocic et al., 2016). These reservoirs are located at a significantly lower depth (4724–5533 m) then the maximum possible storage depth proposed here. The hypothesized reason for this atypical behaviour is a different caprock sealing mechanism, where carbonate caprock initially dissolves when in contact with the carbonic acid (e.g. Luquot and Gouze, 2009; Menke et al., 2017; Lebedev et al., 2017), but later on precipitates again when the pH increases (Stumm and Morgan, 1996), as for instance observed in basalt (Matter et al., 2016), thus plugging the pore throats and essentially providing a true hermetic seal (=zero permeability). These effects should be further studied in the future; however, only a small percentage of target reservoirs fall into this category (Hosa et al., 2011; Miocic et al., 2016).

3. Conclusions and implications

Structural trapping is the primary CO_2 trapping mechanism in CGS (Intergovernmental Panel on Climate Change (IPCC, 2005; Adam, 2001; Underschultz, 2007), and it is thus of key importance to understand in detail how much CO_2 can be stored by this mechanism. Historically, the column heights h of CO_2 (which can be permanently immobilized by a caprock) have been predicted using a capillary force-buoyancy force balance (Eq. (3)). However, more important than the CO_2 column height h is the actual mass of CO_2 (m_{CO2}) which can be disposed by structural trapping. Thus m_{CO2} as a function of depth has been analysed. Importantly, m_{CO2} goes through a maximum at ~1300 m depth, and thus there exists an optimal structural storage depth at ~1300 m.

A second important point made in this paper, based on an advanced analysis of the CO_2-brine density difference $\Delta\rho$, the CO_2-water interfacial tension γ and particularly the CO_2-water-rock contact angle θ, and how these parameters depend on depth (Fig. 1), is the conclusion that for the typical brine salinities, geothermal and hydrostatic gradients assumed here, caprocks below ~2400 m cannot immobilize CO_2 permanently by structural trapping due to wettability reversal (cp. Fig. 1e,f; note that rock can be CO_2-wet depending on pressure and temperature, Iglauer et al., 2015b; Iglauer, 2017). An exception to this may be reservoirs which have a carbonatic seal layer (Miocic et al., 2016), which, as hypothesized here, could be sealed by dissolution-precipitation reactions with the carbonic acid. However, only 5% (1 out of 20) of the CGS projects fall into this exceptional category, while 10% do not pass above maximum depth criterion and another 10% are borderline and should be checked in more detail; most project depths, however, are above the maximum depth (Hosa et al., 2011).

Finally it is noted that at approximately 15,000 m depth density reversal occurs, and CO_2 is heavier than brine (Span and Wagner, 1996; Wagner and Pruss, 2002). Although this would imply a very safe storage mechanism, it appears at this moment that such depths are currently not economically or technically accessible (note that the deepest well ever drilled was 12,262 m deep, drilled by the Soviets during the Cold War race, “Kola Superdeep Borehole”; Digranes et al., 1996; Rabinovich et al., 2012).

These new insights need to be taken into account in reservoir simulations (e.g. Hesse and Woods, 2010; Doughty, 2010; Gershenzon et al., 2015; Green and Ennis-King, 2010; Al-Khdheeawi et al., 2017) so that reliable storage capacity data is predicted, guaranteeing containment security and successful CO_2 geo-sequestration projects.

References

Adam, D., 2001. The North Sea bubble. Nature 411, 518. https://doi.org/10.1038/35079280.

Akhbari, D., Hesse, M.A., 2016. Causes of underpressure in natural CO_2 reservoirs and implications for geological storage. Geology 45 (1), 47–50.

Al-Khdheeawi, E.A., Vialle, S., Barifcani, A., Sarmadivaleh, M., Iglauer, S., 2017. Impact of reservoir wettability and heterogeneity on CO_2-plume migration and trapping capacity. Int. J. Greenh. Gas Control 58, 142–158.

Al-Yaseri, A., Barifcani, A., Lebedev, M., Iglauer, S., 2016a. Receding and advancing CO_2-brine-quartz contact angles as a function of pressure, temperature, surface roughness and salinity. J. Chem. Thermodyn. 93, 416–423.

Al-Yaseri, A., Lebedev, M., Barifcani, A., Iglauer, S., 2016b. Dependence of quartz wettability on fluid density. Geophys. Res. Lett. 43, 3771–3776.

Al-Yaseri, A.Z., Roshan, H., Zhang, Y., Rahman, T., Barifcani, A., Iglauer, S., 2017. Effect of temperature on CO_2/brine/dolomite wettability: hydrophilic versus hydrophobic surfaces. Energy Fuels 31, 6329–6333.

Arif, M., Al-Yaseri, A.Z., Barifcani, A., Lebedev, M., Iglauer, S., 2016a. Impact of pressure and temperature on CO_2-brine-mica contact angles and CO_2-brine interfacial tension: implications for carbon geo-sequestration. J. Colloid Interface Sci. 462, 208–215.

Arif, M., Barifcani, A., Iglauer, S., 2016b. Solid/CO_2 and solid/water interfacial tensions as a function of pressure, temperature, salinity and mineral type: implications for CO_2-wettability and CO_2 geo-storage. Int. J. Greenh. Gas Control 53, 263–273.

Arif, M., Lebedev, M., Barifcani, A., Iglauer, S., 2016c. Structural trapping capacity of oil-wet caprock as a function of pressure, temperature and salinity. Int. J. Greenh. Gas Control 50, 112–120.

Arif, M., Lebedev, M., Barifcani, A., Iglauer, S., 2017. Influence of shale-total organic content on CO_2 geo-storage potential. Geophys. Res. Lett. 44. https://doi.org/10.1002/2019GL073532.

Armitage, P.J., Faulkner, D.R., Worden, R.H., 2013. Caprock corrosion. Nat. Geosci. 6, 79–80. https://doi.org/10.1038/ngeo1716.

Bachu, S., Adams, J.J., 2003. Sequestration of CO_2 in geological media in response to climate change: capacity of deep saline aquifers to sequester CO_2 in solution. Energy Convers. Manage. 44, 3151–3175.

Broseta, D., 2012. Assessing seal rock integrity for CO_2 geological storage purposes. In: Pljaudier-Cabot, G., Pereira, J.M. (Eds.), Geomechanics of CO_2 Storage Facilities. Wiley.

Broseta, D., Tonnet, N., Shah, V., 2012. Are rocks still water-wet in the presence of dense CO_2 or H_2S. Geofluids 12, 280–294.

Busch, A., Alles, S., Gensterblum, Y., Prinz, D., Dewhurst, D.N., Raven, M.D., Stanjek, H., Krooss, B.M., 2008. Carbon dioxide storage potential of shales. Int. J. Greenh. Gas Control 2, 297–308.

Chalbaud, C., Robin, M., Lombard, J.M., Martin, F., Egermann, P., Bertin, H., 2009. Interfacial tension measurements and wettability evaluation for geological CO_2 storage. Adv. Water Resour. 32, 98–109.

Chaudhary, K., Guiltinan, E.J., Bayani Cardenas, M., Maisano, J.A., Ketcham, R.A., Bennett, P.C., 2015. Wettability measurement under high P-T conditions using x-ray imaging with application to the brine-supercritical CO_2 system, geochemistry. Geophys. Geosyst. 16, 2858–2864. https://doi.org/10.1002/2015GC005936.

Chen, C., Zhang, N., Li, W., Song, Y., 2015. Water contact angle dependence with hydroxyl functional groups on silica surfaces under CO_2 sequestration conditions. Environ. Sci. Techol. 49, 14680–14687.

Chilingarian, G.V., Serebryakov, V.A., Robertson, J.O., 2002. Origin and Prediction of Abnormal Formation Pressures. Elsevier, Amsterdam.

Chiquet, P., Broseta, D., Thibeau, S., 2007. Wettability alteration of caprock minerals by carbon dioxide. Geofluids 7, 112–122.

Chun, B.-S., Wilkinson, G.T., 1995. Interfacial tension in high-pressure carbon dioxide mixtures. Ind. Eng. Chem. Res. 34, 4371–4377.

Dake, L.P., 1978. Fundamentals of Reservoir Engineering. Elsevier, Amsterdam.

De Gennes, P.-G., Brochard-Wyart, F., Quere, D., 2004. Capillarity and Wetting Phenomena. Springer, New York.

Dewhurst, D.N., Jones, R.M., Raven, M.D., 2002. Microstructural and petrophysical characterization of muderong shale: application to top seal risking. Pet. Geosci. 8, 371–383.

Dickson, J.L., Gupta, G., Horozov, T.S., Binks, B.P., Johnston, K.P., 2006. Wetting phenomena at the CO_2/water/glass interface. Langmuir 22 (5), 2161–2170.

Digranes, P., Kristoffersen, Y., Karajev, N., 1996. An analysis of shear waves observed in VSP data from the superdeep well at Kola, Russia. Geophys. J. Int. 126, 545–554.

Doughty, C., 2010. Investigation of CO_2 plume behavior for a large-scale pilot test of geologic carbon storage in a saline formation. Transp. Porous Media 82 (1), 49–76.

Espinoza, D.N., Santamarina, J.C., 2010. Water-CO_2-mineral systems: interfacial tension, contact angle, and diffusion – implications to CO_2 geological storage. Water Resour. Res. 46 (7), W0753.

Espinoza, D.N., Santamarina, J.C., 2017. CO_2 breakthrough-caprock sealing efficiency and integrity for carbon geological storage. Int. J. Greenh. Gas Control 66, 218–229.

Farokhpoor, R., Bjørkvik, B.J.A., Lindeberg, E., Torsæter, O., 2013. Wettability behaviour

of CO_2 at storage conditions. Int. J. Greenh. Gas Control 12, 18–25.
Firoozabadi, A., Cheng, P., 2010. Prospects for subsurface CO_2 sequestration. AlChE J. 56 (6), 1398–1405.
Georgiadis, A., Maitland, G., Trusler, J.M., Bismarck, A., 2010. Interfacial tension measurements of the (H_2O+ CO_2) system at elevated pressures and temperatures. J. Chem. Eng. Data 55, 4168–4175.
Gershenzon, N.I., Ritzi Jr, R.W., Dominic, D.F., Soltanian, M., Mehnert, E., Okwen, R.T., 2015. Influence of small-scale fluvial architecture on CO_2 trapping processes in deep brine reservoirs. Water Resour. Res. 51 (10), 8240–8256.
Green, C.P., Ennis-King, J., 2010. Effect of vertical heterogeneity on long-term migration of CO_2 in saline formations. Transp. Porous Media 82 (1), 31–47.
Guiltinan, E.J., Bayani Cardenas, M., Bennett, P.C., Zhang, T., Espinoza, D.N., 2017. The effect of organic matter and thermal maturity on the wettability of supercritical CO_2 on organic shales. Int. J. Greenh. Gas Control 65, 15–22.
Hebach, A., Oberhof, A., Dahmen, N., Kogel, A., Ederer, H., Dinjus, E., 2002. Interfacial tension at elevated pressures-measurements and correlations in the water + carbon dioxide system. J. Chem. Eng. Data 47, 1540–1546.
Hesse, M.A., Woods, A.W., 2010. Buoyant dispersal of CO_2 during geological storage. Geophys. Res. Lett. 37, L01403. https://doi.org/10.1029/2009GL041128.
Hesse, M.A., Orr, F.M., Tchelepi, H.A., 2008. Gravity currents with residual trapping. J. Fluid Mech. 611, 35–60.
Hosa, A., Esentia, M., Sewart, J., Haszeldine, S., 2011. Injection of CO_2 into saline formations: benchmarking worldwide projects. Chem. Eng. Res. Des. 89, 1855–1864.
Iglauer, S., 2017. CO_2-water-rock wettability: variability, influencing factors, and implications for CO_2 geostorage. Acc. Chem. Res. 50, 1134–1142.
Iglauer, S., Mathew, M., Bresme, F., 2012. Molecular dynamics computations of brine-CO_2 interfacial tensions and brine-CO_2-quartz contact angles and their effects on structural and residual trapping mechanisms in carbon geo-sequestration. J. Colloid Interface Sci. 386, 405–414.
Iglauer, S., Hassan, A., Sarmadivaleh, M., Liu, K., Phan, C., 2014. Contamination of silica surfaces: impact on water-CO_2-quartz and glass contact angle measurements. Int. J. Greenh. Gas Control 22, 325–328.
Iglauer, S., Al-Yaseri, A.Z., Rezaee, R., Lebedev, M., 2015a. CO_2-wettability of caprocks: implications for structural storage capacity and containment security. Geophys. Res. Lett. 42, 9279–9284.
Iglauer, S., Pentland, C.H., Busch, A., 2015b. CO_2-wettability of seal and reservoir rocks and the implications for carbon geo-sequestration. Water Resour. Res. 51 (1), 729–774. https://doi.org/10.1002/wrcr.21095. WR015553.
Intergovernmental Panel on Climate Change (IPCC), 2005. IPCC Special Report on Carbon Dioxide Capture and Storage, Prepared by Working Group III of the Intergovernmental Panel on Climate Change. Cambridge University Press.
Jung, J.-W., Wang, J., 2012. Supercritical CO_2 and ionic strength effects on wettability of silica surfaces: equilibrium contact angle measurements. Energy Fuels 26, 6053–6059.
Lackner, K.S., 2003. Climate change. A guide to CO_2 sequestration. Science (80-) 300, 1677–1678. https://doi.org/10.1126/science.1079033.
Lebedev, M., Zhang, Y., Sarmadivaleh, M., Barifcani, A., Iglauer, S., 2017. Carbon geosequestration in limestone: pore-scale dissolution and geomechanical weakening. Int. J. Greenh. Gas Control. 66, 106–119.
Li, Z., Dong, M., Li, S., Huang, S., 2006. CO_2 sequestration in depleted oil and gas reservoirs – caprock characterization and storage capacity. Energy Convers. Manage. 47, 1372–1382.
Li, Y., Pham, J.Q., Johnston, K.P., Green, P.F., 2007. Contact angle of water on polystyrene thin films: effects of CO_2 environment and film thickness. Langmuir 23, 9785–9793.
Li, X., Boek, E., Maitland, G.C., Trusler, J.P.M., 2012a. Interfacial tension of (brines + CO_2): (0.864 NaCl + 0.136 KCl) at temperatures between (298 and 448) K, pressures between (2 and 50) MPa, and total molalities of (1 to 5) mol kg-1. J. Chem. Eng. Data 57 (4), 1078–1088. https://doi.org/10.1021/je201062r.
Li, X., Boek, E., Maitland, G.C., Trusler, J.P.M., 2012b. Interfacial tension of (brines + CO_2): $CaCl_2$ (aq), $MgCl_2$ (aq), and $NaSO_4$ (aq) at temperatures between (343 and 423) K, pressures between (2 and 50) MPa, and molalities of (0.5 to 5) mol·kg-1. J. Chem. Eng. Data 57, 1369–1375.
Liang, Y., Tsuji, S., Jia, J., Tsuji, T., Matsuoka, T., 2017. Modeling CO_2-water-mineral wettability and mineralization for carbon geosequestration. Acc. Chem. Res. 50 (7), 1530–1540.
Luquot, L., Gouze, P., 2009. Experimental determination of porosity and permeability changes induced by injection of CO_2 into carbonate rocks. Chem. Geol. 265, 1–2 1480159.
Matter, J.M., Stute, M., Snaebjoernsdottir, S.O., Oelkers, E.H., Gislason, S.R., Aradottir, E.S., Sigfusson, B., Gunnarsson, I., Sigurdardottir, H., Gunnlaugsson, E., Axelsson, G., Alfredsson, H.A., Wolff-Boensich, D., Mesfin, K., De la, Reguera, Taya, D.F., Hall, J., Dideriksen, K., Broecker, W.S., 2016. Rapid carbon mineralization for permanent disposal of anthropogenic carbon dioxide emissions. Science (80-) 352, 1312–1314.
Meckel, T.A., 2010. Capillary seals for trapping carbon dioxide (CO_2) in underground reservoirs. Developments and Innovation in Carbon Dioxide (CO_2) Caputre and Storage Technology: Carbon Dioxide (CO_2) Storage and Utilization, vol. 2.
Menke, H.P., Bijeljic, B., Blunt, M.J., 2017. Dynamic Reservoir-condition microtomography of reactive transport in complex carbonates: effect of initial Pore structure and initial brine pH. Geochim. Cosmochim. Acta 204, 267–285. https://doi.org/10.1016/j.gca.2017.01.053.
Miocic, J.M., Gilfillan, S.M.V., Roberts, J.J., Edlmann, K., McDermott, C.I., Haszeldine, R.S., 2016. Controls on CO_2 storage security in natural reservoirs and implications fir CO_2 storage site selection. Int. J. Greenh. Gas Control 51, 118–125.
Naylor, M., Wilkinson, M., Haszeldine, R.S., 2011. Calculation of CO_2 column height in depleted gas fields from known pre-production gas column heights. Mar. Pet. Geol. 28, 1083–1093.
Nelson, P.H., 2009. Pore-throat sizes in sandstones, tight sandstones, and shales. AAPG Bull. 93 (3), 329–340.
Orr, F.M., 2009. Onshore geologic storage of CO_2. Science (80-) 325, 1656–1658. https://doi.org/10.1126/science.1175677.
Pan, B., Li, Y., Wang, H., Jones, F., Iglauer, S., 2018. CO_2 and CH_4 wettabilities of organic-rich shale. Energy Fuels 32, 1914–1922.
Park, J.-Y., Lim, J.S., Yoon, C.H., Lee, C.H., Park, K.P., 2005. Effect of a fluorinated sodium bis(2-ethylhexyl) sulfosuccinate (aerosol-OT, AOT) analogue surfactant onn the interfacial tension CO_2 + water and CO_2 + Ni-plating solution in near- and supercritical CO_2. J. Chem. Eng. Data 50, 299–308.
Rabinovich, G.Y., Aptikaeva, O.I., Gamburtsev, A.G., 2012. Evidence of geodynamical processes in the ancient crust from the seismoacoustic model of the kola superdeep borehole. Phys. Chem. Earth Part A Solid Earth Geod. 48 (11-12), 850–858.
Riaz, A., Hesse, M., Tchelepi, H.A., Orr, F.M., 2006. Onset of convection in a gravitationally unstable diffusive boundary layer in porous media. J. Fluid Mech. 548, 87–111.
Roshan, H., Al-Yaseri, A.Z., Sarmadivaleh, M., Iglauer, S., 2016. On wettability of shale rocks. J. Colloids Interface Sci. 475, 104–111.
Saraji, S., Goual, L., Piri, M., Plancher, H., 2013. Wettability of supercritical carbon dioxide/water/quartz systems: simultaneous measurement of contact angle and interfacial tension at reservoir conditions. Langmuir 29, 6856–6866.
Sarmadivaleh, M., Al-Yaseri, A.Z., Iglauer, S., 2015. Influence of temperature and pressure on quartz-water-CO_2 contact angle and CO_2-water interfacial tension. J. Colloid Interface Sci. 441, 59–64. https://doi.org/10.1016/j.jcis.2014.11.010.
Shojai Kaveh, N.S., Rudolph, E.S.J., Van Hemert, P., Rossen, W.R., Wolf, K.H., 2014. Wettability evaluation of a CO_2/water/Bentheimer sandstone system: contact angle, dissolution, and bubble size. Energy Fuel 28 (6), 4002–4020.
Shojai Kaveh, N.S., Barnhoorn, A., Wolf, K.H., 2016. Wettability evaluation of silty shale caprocks for CO_2 storage. Int. J. Greenh. Gas Control 49, 425–435.
Song, J., Zhang, D., 2013. Comprehensive review of caprock-sealing mechanisms for geologic carbon sequestration. Environ. Sci. Technol. 47, 9–22.
Span, R., Wagner, W., 1996. A New equation of State for carbon dioxide covering the fluid region from the triple-point temperature to 1100 K at pressures up to 800 MPa. J. Phys. Chem. Ref. Data 25 (6), 1509–1596. https://doi.org/10.1063/1.555991.
Stumm, W., Morgan, J.J., 1996. Aquatic Chemistry. Wiley, New York.
Thompson, A.H., Katz, A.J., Raschke, R.A., 1987. Mercury injection in porous media: a resistance devil's staircase with percolation geometry. Phys. Rev. Lett. 58 (1), 29–32. https://doi.org/10.1103/PhysRevLett.58.29.
Underschultz, J., 2007. Hydrodynamics and membrane seal capacity. Geofluids 7, 148–158.
Vernik, L., Milovac, J., 2011. Rock physics of organic shales. Lead. Edge 30 (3), 318–323.
Wagner, W., Pruss, A., 2002. The IAPWS formulation 1995 for the thermodynamic properties of ordinary water substance for general and scientific use. J. Phys. Chem. Ref. Data 31 (2), 387–535. https://doi.org/10.1063/1.1461829.
Wollenweber, J., Alles, S., Busch, A., Krooss, B.M., Stanjek, H., Littke, R., 2010. Experimental investigation of the CO_2 sealing efficiency of caprocks. Int. J. Greenh. Gas Control 4, 231–241. https://doi.org/10.1016/j.ijggc.2010.01.003.
Xie, X., Fan, Z., Liu, X., Lu, Y., 2006. Geochemistry of formation water and its implication on overpressured fluid flow in the Dongying depression of the Bohaiwan Basin, China. Geochem. Explor. Environ. Anal. 89, 432–435.
Yang, D., Gu, Y., Tontiwachwuthikul, P., 2008. Wettability determination of the reservoir brine - reservoir rock system with dissolution of CO_2 at high pressures and elevated temperatures. Energy Fuels 22 (1), 504–509.